JAIST Repository
https://dspace.jaist.ac.jp/

Title	Drastic suppression of the optical reflection of flash-lamp-crystallized poly-Si films with spontaneously formed periodic microstructures
Author(s)	Ohdaira, Keisuke; Nishikawa, Takuya; Shiba, Kazuhiro; Takemoto, Hiroyuki; Matsumura, Hideki
Citation	Thin Solid Films, 518(21): 6061-6065
Issue Date	2010
Type	Journal Article
Text version	author
URL	http://hdl.handle.net/10119/9882
Rights	NOTICE: This is the author's version of a work accepted for publication by Elsevier. Keisuke Ohdaira, Takuya Nishikawa, Kazuhiro Shiba, Hiroyuki Takemoto, and Hideki Matsumura, Thin Solid Films, 518(21), 2010, 6061-6065, http://dx.doi.org/10.1016/j.tsf.2010.05.115
Description	

Japan Advanced Institute of Science and Technology

Drastic suppression of the optical reflection of flash-lamp-crystallized poly-Si films with spontaneously formed periodic microstructures

Keisuke Ohdaira, Takuya Nishikawa, Kazuhiro Shiba, Hiroyuki Takemoto,

and Hideki Matsumura

Japan Advanced Institute of Science and Technology (JAIST)

1-1 Asahidai, Nomi, Ishikawa 923-1292, Japan

Tel: +81-761-51-1563, Fax: +81-761-51-1149, E-mail: ohdaira@jaist.ac.jp

Polycrystalline Si (poly-Si) films formed by flash lamp annealing of precursor a-Si films on glass substrates have periodic surface roughness spontaneously formed through crystallization, which effectively acts to decrease optical reflection. The surface roughness initially decreases, and then reversely increases with increase in the duration of wet etching, performed to modulate the surface morphology and to reduce optical reflectance. This curious phenomenon can be understood as the selective removal of surface projections, which contain a number of voids, and as different etching rates of large-grain and fine-grain regions. The antireflection effect is enhanced not by the variation of the surface roughness, but rather by the removal of the voids near the surface. The etched poly-Si films covered with antireflection films show remarkably low average reflectance of 3% without any complicated texturing processes, which will lead to the fabrication of high-efficiency solar cells by a simple process.

KEYWORDS: flash lamp annealing, crystallization, reflectance, polycrystalline silicon, solar cell, antireflection

1. Introduction

Crystalline Si (c-Si) solar cells, formed using bulk c-Si wafers, are most widely used because of their mature fabrication processes and long-term stable operation. The quantity of Si used in the fabrication of c-Si solar cells is, however, still large, in spite of diligent efforts to eliminate kerf loss during slicing and to cut ingots as thin as possible [1,2]. From the viewpoint of Si usage, thin-film Si solar cells, fabricated using Si films such as amorphous Si (a-Si) and microcrystalline Si (μc-Si) deposited by chemical vapor deposition (CVD), are of great advantage. One of the most serious problems of Si thin-film solar cells is relatively low conversion efficiency, because of low carrier mobility and the resultant short carrier diffusion length. To provide both the advantages of long carrier lifetime in c-Si and efficient Si usage, polycrystalline Si (poly-Si) films with high crystalline fraction have attracted attention as next-generation solar cell material [3-6]. Thin-film poly-Si solar cells with more than 10% conversion efficiency have been demonstrated, indicating high feasibility of this concept [3]. However, most approaches for poly-Si formation require a high-temperature process, at 600 °C or more, negating the possibility of using conventional, cost-effective soda lime glass substrates with glass transition temperature of less than 600 °C. Non-thermal equilibrium treatment will therefore be a key technology to heat precursor a-Si films up to a sufficiently high temperature for crystallization, while avoiding thermal damage to glass substrates.

Flash lamp annealing (FLA) is a millisecond-order annealing technique [7-9], and thus can realize crystallization of a-Si films more than 1 μm thick without any serious peeling of Si films on quartz and soda lime glass substrates, when Cr adhesion films are inserted between Si and glass [10,11]. We have also fabricated solar cells using

poly-Si films formed on glass substrates, and we have demonstrated actual diode and solar cell operation [12], meaning that the poly-Si films formed by FLA on glass substrates can be a candidate for a material utilized in the next-generation thin-film poly-Si solar cells. Effective antireflection structures must be introduced in the solar cell structure for the further improvement of the solar cell properties. Poly-Si films formed by FLA on glass substrates with reactive-ion-etching-textured surfaces, aimed at improvement of optical confinement, however, show worse minority carrier lifetime than those formed on flat substrates, probably due to voids existing inside the poly-Si as well as in the vicinity of the Si/Cr interface [13]. We therefore need to fabricate antireflection structures on the surface of the poly-Si films formed on flat substrates. Fortunately, there exist grating-like periodic structures on poly-Si surfaces, which are spontaneously formed through crystallization by FLA as a result of lateral explosive crystallization [14,15]. These characteristic structures act to reduce optical reflectance to some extent, and further enhancement of antireflection will be realized by modulating these surface structures.

In this paper, we investigate the variation of surface morphology of flash-lamp-crystallized poly-Si films induced by conventional wet chemical etching, and the variations in their optical reflectance. The surface roughness shows complicated variations with changes in etching time. These variations are strongly related to the characteristic microstructure of the poly-Si films. Optical reflectance of the poly-Si films drastically decreases after slight wet etching, and decreases even more after antireflection film formation, resulting in average reflectance of as low as 3%.

2. Experimental details

Cr films 60-200 nm thick were first formed by sputtering on quartz glass substrates 20×20 mm^2 in size. We confirmed no significant change in the microstructure of the crystallized Si films due to variations of Cr film thickness. Precursor a-Si films 4.5 μm thick were then deposited on the Cr-coated substrates by catalytic CVD (Cat-CVD), often called hot-wire CVD. The Cat-CVD can yield a-Si films with hydrogen content of as low as 3%, preventing peeling of the Si films during FLA even without a prior dehydrogenation process [16]. The deposition of a-Si films was performed using SiH_4 and H_2 with flow rates of 50 and 10 sccm, respectively, at a substrate temperature of 320 °C with a deposition rate of approximately 100 nm/min. Further detailed deposition conditions are summarized elsewhere [17]. Flash lamp light was supplied from a Xe lamp array with a sufficient areal homogeneity over a 20×20 mm^2 sample area. Flash lamp light has a broad spectrum mainly in a visible range, whose typical spectrum can be seen elsewhere [18]. FLA was performed under a fixed pulse duration of 5 ms, whereas its irradiance was optimized to maximize the crystallization area around 20 J/cm^2. Only one shot of flash irradiation was supplied for each sample. No additional heating was performed during FLA.

The poly-Si films were chemically etched by conventional mixed acid in the proportion HF (50%) : HNO_3 (70%) = 1:49 for a duration of up to 60 s at room temperature. Indium tin oxide (ITO) films 100 nm thick were formed by sputtering on some of the etched poly-Si films to form an antireflection coating. The etching rate of the poly-Si films with the mixed acid is approximately 30 nm/s. The microstructures of etched poly-Si films were characterized by atomic force microscopy (AFM) (Veeco Instruments Inc., Nanoscope III) with tapping mode using a cantilever whose thickness, length, and width are 4, 125, and 30 μm, respectively, and transmission electron

microscopy (TEM) operated at a acceleration voltage of 200 kV. The surface root-mean-square (RMS) roughness of the poly-Si films was estimated from 10×10 μm^2-area AFM images. The spectral reflectance of wet-etched poly-Si films was measured with a spectrophotometer (SHIMAZU Co. Ltd., UV-3150) equipped with an integrating sphere.

3. Results and discussion

Figure 1 shows the surface AFM images of the poly-Si films before and after wet etching of various durations. The 1-μm-spaced grating-like periodic structures can be clearly seen in the image of the poly-Si film before etching. The RMS roughness is as high as approximately 120 nm, as has been already reported [14]. As the etching progresses, the surface morphology of the poly-Si films changes drastically, while maintaining the original stripe patterns. Figure 2 shows the RMS roughness of the poly-Si surface as a function of etching time. Interestingly, the roughness first decreases with etching time, and then reversely increases and finally exceeds the initial RMS roughness, in spite of using the etchant conventionally used for mirror etching of Si. This phenomenon is strongly related to the microstructure of the flash-lamp-crystallized poly-Si films. Figure 3 shows the cross-sectional TEM image of a flash-lamp-crystallized poly-Si film. The periodic surface roughness can be seen on the surface, along with a large number of voids just below the surface projections. There also exist periodic structures consisting of two different grain-size regions inside the poly-Si film. One is the large-grain region, containing relatively large grains more than 100 μm in size, which is connected to the surface projections. The other is the fine-grain region, consisting only of 10-nm size small grains, linked to the flat regions

of the surface. The fact of the existence of 10-nm-size fine grains is consistent with the line width of the Raman c-Si peak of 7-9 cm^{-1} shown previously [7,8]. The mechanism of the formation of these characteristic periodic microstructures has been discussed elsewhere in detail [15], and we concentrate our attention here in this paper on the variations of the surface morphology and of their optical reflectance. Based on the characteristic microstructures, the seemingly complicated variations of surface roughness with the etching process can be fully understood as follows. Figure 4 shows the schematics of the structural variations of the poly-Si films due to wet etching. In the initial stage, the projecting regions, containing a large number of voids, will be etched more rapidly, resulting in decreased surface roughness. However, in the second stage, that is, after the removal of the surface voids, the fine-grain regions are etched faster than the large-grain regions, because of the existence of more grain boundaries. This phenomenon increases the surface roughness. This explanation is supported by the cross-sectional TEM image of the poly-Si film after 60-s etching shown in Fig. 5. The periodic surface structure has been kept, and the large-grain regions are still projecting, even after removal of 1.8-μm-thick poly-Si from the surface.

Figure 6 shows the optical reflectance spectra of the poly-Si films after wet etching of durations up to 60 s, along with the spectrum of a mirror-polished flash-lamp-crystallized poly-Si film for comparison. Note that the mirror-polished poly-Si film has higher reflectance than the unpolished ones, which clearly indicates that surface roughness effectively acts to decrease surface optical reflectance. With increased etching time, optical reflectance decreases in the whole visible range. The variations of the average optical reflectance as a function of etching time are summarized in Fig. 7. The RMS roughness of the poly-Si films, already shown in Fig.

2, is again plotted for comparison with the reflectance variation. Optical reflectance in general decreases with increased surface roughness, which is not the case with the flash-lamp-crystallized poly-Si films, for the two reasons that reflectance decreases with decrease in RMS roughness, and that reflectance plateaus even after increase in the roughness. These phenomena can be understood as follows. Some of voids, existing near the surface, would act to increase optical reflection, since they can reflect some incident photons due to the different refractive indices of air and c-Si if the voids have a dimension larger than or similar to the wavelength of incident light. Besides that, we should consider the possibility of antireflection due to the formation of a subwavelength structure (SWS) [19]. The surface structures might act as SWS due to their periodicity and dimension, and the reflection of incident light could be dominated by the variation of average refractive index from the top to the bottom of the surface structure. Surface voids contribute to reduction in the average refractive index of the projecting region, resulting in its reflective index closer to air. The removal of voids by etching would lead to more gradual variation of refractive index from air to c-Si and the resultant suppression of optical reflection. On the basis of these considerations, the initial drop in optical reflectance, shown in Fig. 7, is probably not related to the variations of surface roughness, but caused by the removal of the surface voids. This effect will continue until the surface void-containing regions are completely etched off. The etching time of 15 s, required to minimize average reflectance, corresponds to an etching thickness of approximately 450 nm, which roughly equals the depth of voids, as shown in Fig. 3. The least RMS roughness (approximately 50 nm) shown in Fig. 2, realized after 15-s etching, corresponds to more than 100 nm height from the bottom to the top of the projections, which seems to be large enough for sufficient antireflection.

With sufficiently high projections, most incoming photons between the projections will be absorbed, and only the photons colliding with the tops of the projections will be reflected.

Finally, we discuss the benefits of the spontaneously-formed roughness structures, and of the resulting antireflection effects. Figure 8 shows the reflectance spectra of the poly-Si films before and after formation of an ITO antireflection film on the poly-Si films etched for 60 s, along with the spectra of the as-crystallized poly-Si films without and with ITO film coating for comparison. Optical reflectance of the etched poly-Si film significantly decreases after ITO film formation, resulting in an average reflectance of as low as 3%. The ITO films are necessary for the front electrodes of the final solar cell structure, and hence, the solar cells fabricated using etched poly-Si films actually have such low reflectance. Since the surface void-containing regions are etched off, a doped layer must be formed on top of the structured surface after the wet etching process, for instance, by some deposition techniques. Although the fabrication process of solar cells becomes complicated, the solar cell performance can be improved in the post-deposition process, because surface passivation layers, such as thin intrinsic a-Si layers, can be inserted between the etched poly-Si films and doping layers [20]. Low RMS roughness is probably better for good surface coverage with post-deposited doping layers and with ITO films [21]. The fact that the poly-Si films with the lowest RMS roughness also have the lowest reflectance is therefore quite favorable to realizing high-efficiency solar cells. The periodic surface structures provide another advantage when the poly-Si films are used as the bottom layer of tandem solar cells. The top layers are deposited on the rough poly-Si films, which will significantly enhance optical confinement in the top layers. Recently, purposely formed grating structures on glass

substrates have been used to demonstrate enhancement of light trapping through changing the grating period and height [22]. Since such grating structures are spontaneously formed on flash-lamp-crystallized poly-Si films without any complicated processes, additional light-trapping effects are expected both in the poly-Si layers and in the top layers.

4. Conclusions

We demonstrate drastic reduction of optical reflectance in flash-lamp-crystallized poly-Si films by conventional wet chemical etching. The surface roughness shows curious changes with etching time, which can be fully understood by considering the characteristic microstructures of the poly-Si films, which consist of void-containing projections and of two different grain-size regions. Optical reflectance suddenly decreases, and then, plateaus with increase in etching time, indicating that reflectance is reduced by the removal of a large number of voids near the surface. By combining reflection-suppressing etching and the ITO antireflection film coating, the average optical reflectance of the poly-Si films can be decreased down to as low as 3% without any complicated processes, which will contribute to improvement in solar cell performance.

Acknowledgments

The authors acknowledge T. Owada and T. Yokomori of Ushio Inc. for their expert operation of FLA, and T. Miyazaki and T. Genko of JAIST for their assistance in the AFM measurement. We also would like to thank Prof. M. A. Mooradian of JAIST for her English correction.

References

[1] F. Dross, A. Milhe, J. Robbelein, I. Gordon, P.-O. Bouchard, G. Beaucarne, J. Poortmans, Proceedings of the 23rd European Photovoltaic Solar Energy Conference, Valencia, Spain, September 1-5, 2008, p. 1278.

[2] F. Henley, A. Lamm, S. Kang, Z. Liu, L. Tian, Proceedings of the 23rd European Photovoltaic Solar Energy Conference, Valencia, Spain, September 1-5, 2008, p. 1090.

[3] M. J. Keevers, T. L. Young, U. Schubert, M. A. Green, Proceedings of the 22nd European Photovoltaic Solar Energy Conference, Milan, Italy, September 3-7, 2007, p. 1783, and references therein.

[4] I. Gordon, D. Van Gestel, L. Carnel, G. Beaucarne, J. Poortmans, K. Y. Lee, P. Dogan, B. Gorka, C. Becker, F. Fenske, B. Rau, S. Gall, B. Rech, J. Plentz, F. Falk, D. Le Bellac, Proceedings of the 22nd European Photovoltaic Solar Energy Conference, Milan, Italy, September 3-7, 2007, p. 1890, and references therein.

[5] S. Janz, M. Kuenle, S. Lindekugel, E.J. Mitchell, S. Reber, Proceedings of the 33rd IEEE Photovoltaic Specialists Conference, San Diego, U.S.A., May 11-16, 2008, p. 1805, and references therein.

[6] K. Y. Lee, C. Becker, M. Muske, F. Ruske, S. Gall, B. Rech, M. Berginski, J. Hüpkes, Appl. Phys. Lett. **91** (2007) 241911.

[7] F. Terai, S. Matsunaka, A. Tauchi, C. Ichikawa, T. Nagatomo, T. Homma, J. Electrochem. Soc. **153** (2006) H147.

[8] B. Pétz, L. Dobos, D. Panknin, W. Skorupa, C. Lioutas, N. Vouroutzis, Appl. Surf. Sci. **242** (2005) 185.

[9] M. Smith, R. McMahon, M. Voelskow, D. Panknin, W. Skorupa, J. Cryst. Growth **285** (2005) 249.

[10] K. Ohdaira, Y. Endo, T. Fujiwara, S. Nishizaki, H. Matsumura, Jpn. J. Appl. Phys. **46** (2007) 7603.

[11] K. Ohdaira, T. Fujiwara, Y. Endo, S. Nishizaki, H. Matsumura, Jpn. J. Appl. Phys. **47** (2008) 8239.

[12] K. Ohdaira, T. Fujiwara, Y. Endo, K. Shiba, H. Takemoto, S. Nishizaki, Y. R. Jang, K. Nishioka, H. Matsumura, Proceedings of the 33rd IEEE Photovoltaic Specialists Conference, San Diego, U.S.A., May 11-16, 2008, p. 1690.

[13] K. Ohdaira, T. Fujiwara, Y. Endo, K. Nishioka, H. Matsumura, J. Cryst. Growth **311** (2009) 769.

[14] K. Ohdaira, T. Fujiwara, Y. Endo, S. Nishizaki, K. Nishioka, H. Matsumura, Technical Digest of the 17th International Photovoltaic Science and Engineering Conference, Fukuoka, Japan, December 3-7, 2007, p. 1326.

[15] K. Ohdaira, T. Fujiwara, Y. Endo, S. Nishizaki, H. Matsumura, J. Appl. Phys. **106** (2009) 044907.

[16] K. Ohdaira, K. Shiba, H. Takemoto, T. Fujiwara, Y. Endo, S. Nishizaki, Y. R. Jang, H. Matsumura, Thin Solid Films **517** (2009) 3472.

[17] K. Ohdaira, S. Nishizaki, Y. Endo, T. Fujiwara, N. Usami, K. Nakajima, H. Matsumura, Jpn. J. Appl. Phys. **46** (2007) 7198.

[18] H. Habuka, A. Hara, T. Karasawa, and M. Yoshioka, Jpn. J. Appl. Phys. **46** (2007) 937.

[19] H. Sai, H. Fujii, K. Arafune, Y. Ohshita, M. Yamaguchi, Y. Kanamori and H. Yugami, Appl. Phys. Lett. **88** (2006) 201116.

[20] K. Ohdaira, Y. Endo, T. Fujiwara, K. Shiba, H. Takemoto, K. Koyama, S. Nishizaki, Y. R. Jang, K. Nishioka, H. Matsumura, Proceedings of the 23rd European Photovoltaic Solar Energy Conference, Valencia, Spain, September 1-5, 2008, p. 2042.

[21] K. Ohdaira, H. Takemoto, K. Shiba, T. Nishikawa, K. Koyama, and H. Matsumura, Proceedings of the 34th IEEE Photovoltaic Specialists Conference, Philadelphia, U.S.A., June 7-12, 2009, p. 26.

[22] O. Isabella, A. Campa, M. C. R. Heijna, W. Soppe, R. van Erven, R. H. Franken, H. Borg, M. Zeman, Proceedings of the 23rd European Photovoltaic Solar Energy Conference, Valencia, Spain, September 1-5, 2008, p. 2320.

Figure captions

Fig. 1 AFM images of the flash-lamp-crystallized poly-Si surfaces with an area of 10×10 μm^2 after (a) 0-, (b) 15-, and (c) 60-s etching.

Fig. 2 RMS roughness of the flash-lamp-crystallized poly-Si films as a function of etching time.

Fig. 3 Cross-sectional TEM image of the flash-lamp-crystallized poly-Si film. Solid and dashed arrows indicate “Large-grain region” and “Fine-grain region”, respectively. Surface periodic projections are also seen on top of the large-grain regions.

Fig. 4 Schematic diagrams showing the mechanisms of roughness variations of the poly-Si surface due to wet etching.

Fig. 5 Cross-sectional TEM image of the 60-s etched poly-Si film. Dashed squares indicate large-grain regions.

Fig. 6 Optical reflectance spectra of the poly-Si films after wet etching of various durations up to 60 s. The spectrum of the mirror-polished poly-Si film is also plotted for comparison.

Fig. 7 Average optical reflectance of the poly-Si films as a function of etching time. The variation of the RMS roughness is also shown, to emphasize its relation to optical reflectance.

Fig. 8 Optical reflectance spectra of the poly-Si films before and after ITO antireflection film formation. The spectra of the as-crystallized poly-Si films without and with ITO film coating are also shown for comparison.

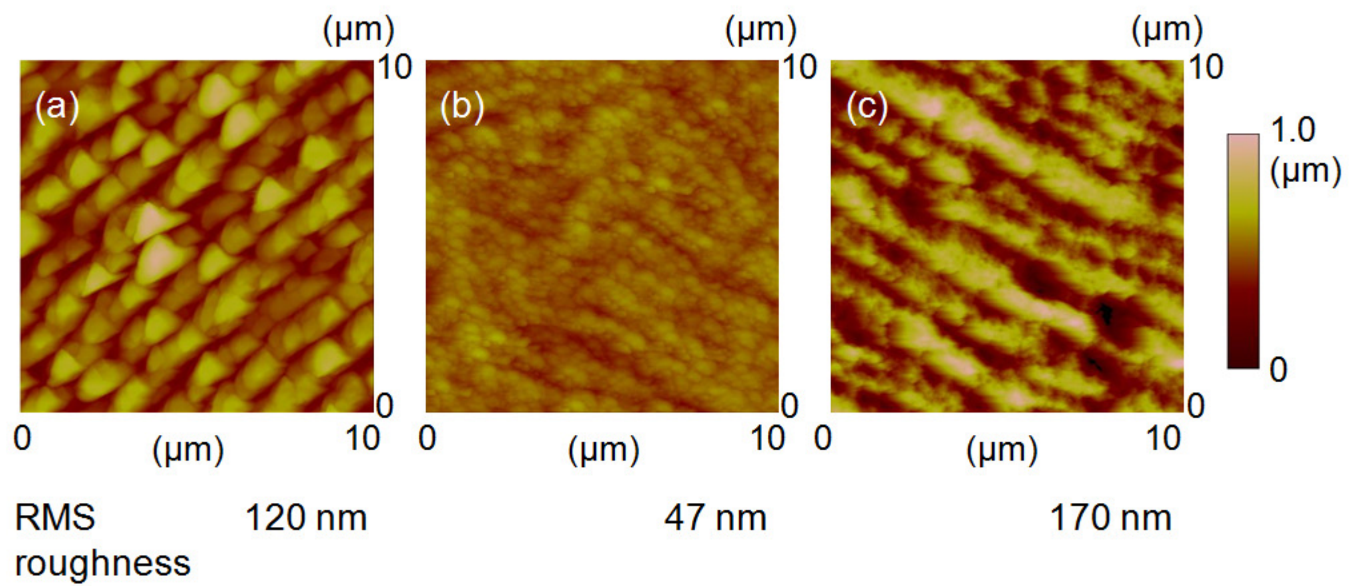

Figure 1 K. Ohdaira *et al*.,

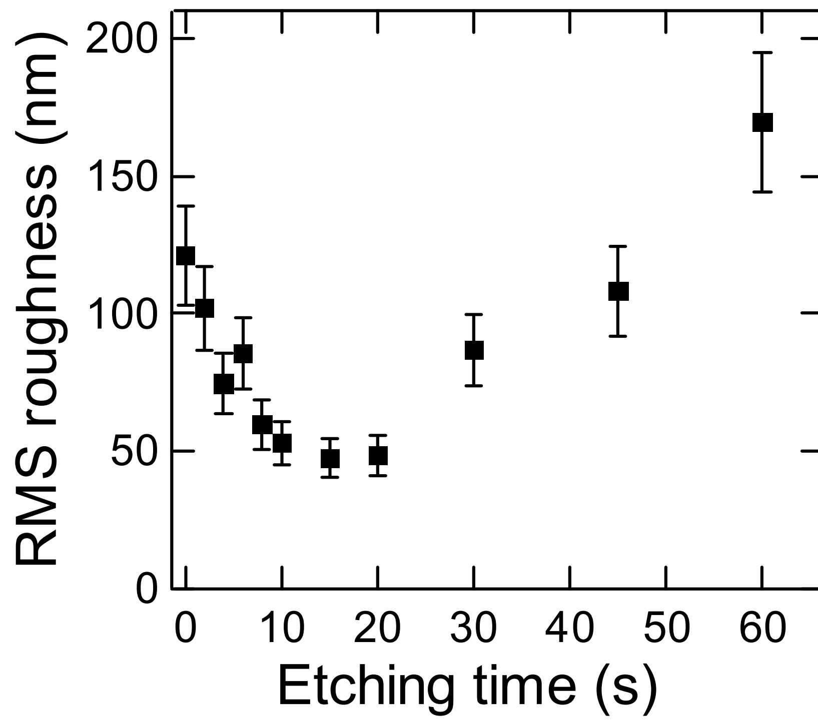

Figure 2 K. Ohdaira *et al.*,

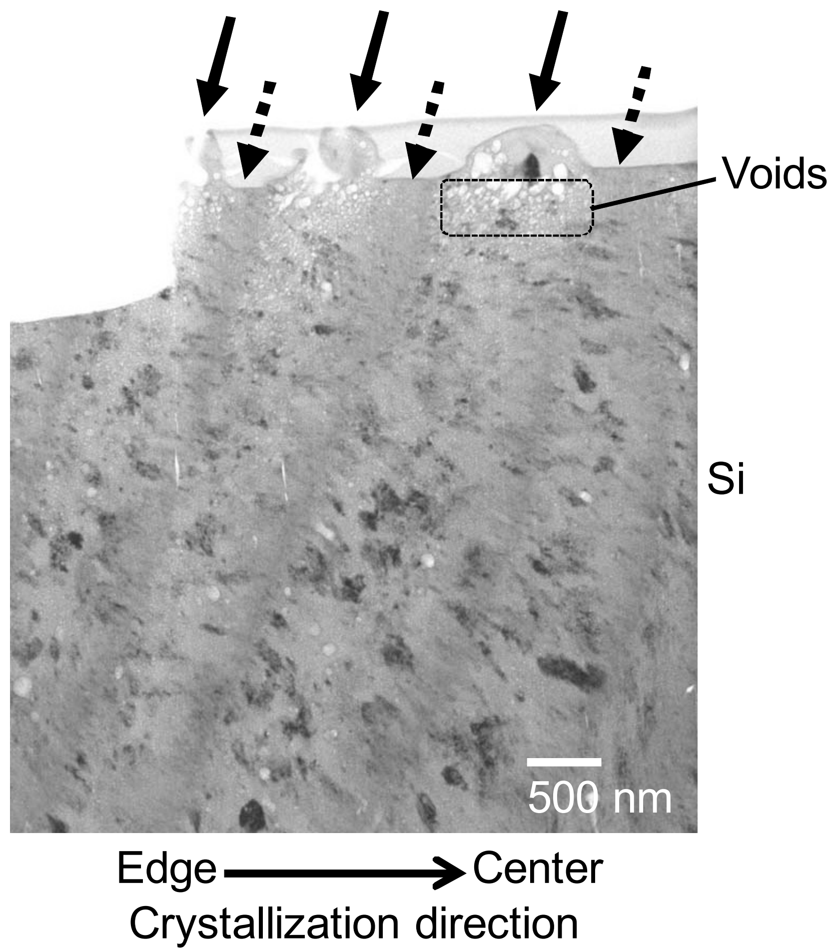

Figure 3 K. Ohdaira *et al*.,

Initial stage

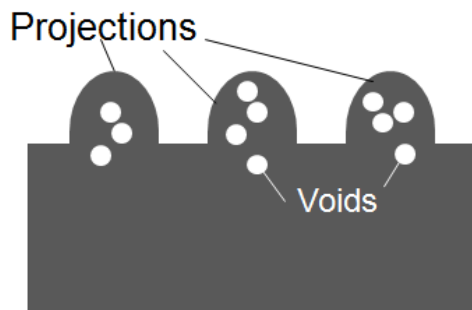

Etching

Selective etching of
void-containing projections
→ Decrease in roughness

Second stage

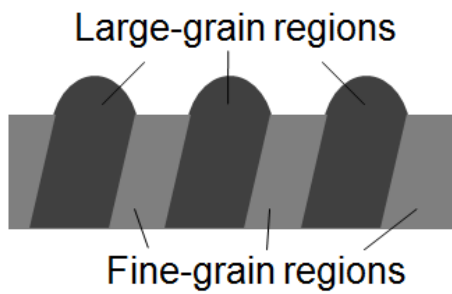

Etching

Faster etching rate of
fine-grain region
→ Increase in roughness

Figure 4 K. Ohdaira *et al.*,

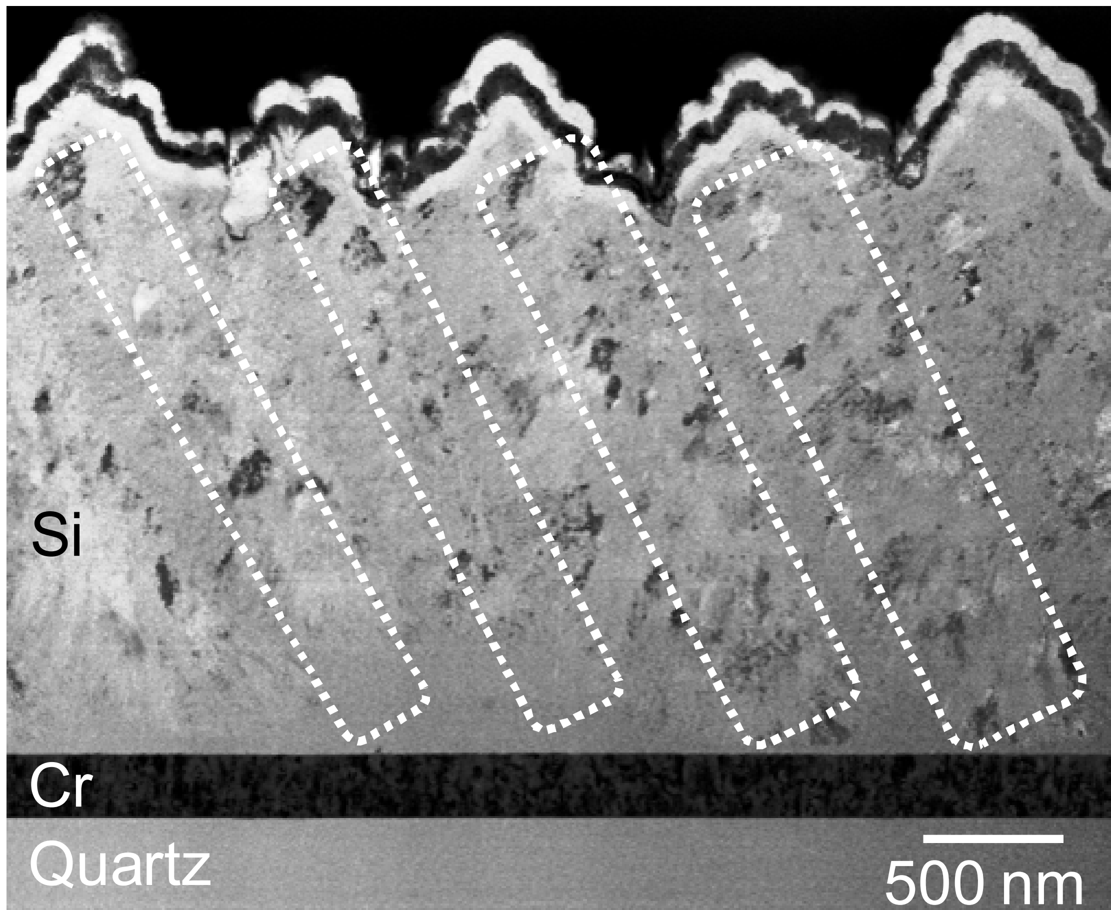

Figure 5 K. Ohdaira *et al*.,

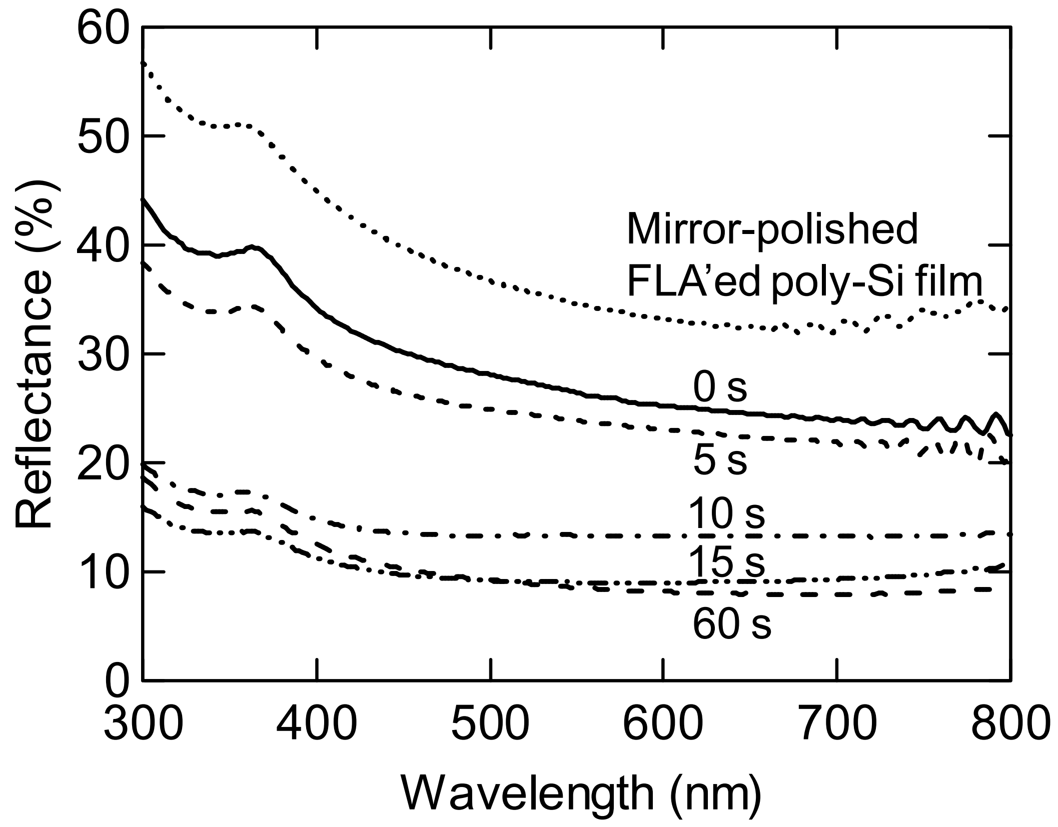

Figure 6 K. Ohdaira *et al*.,

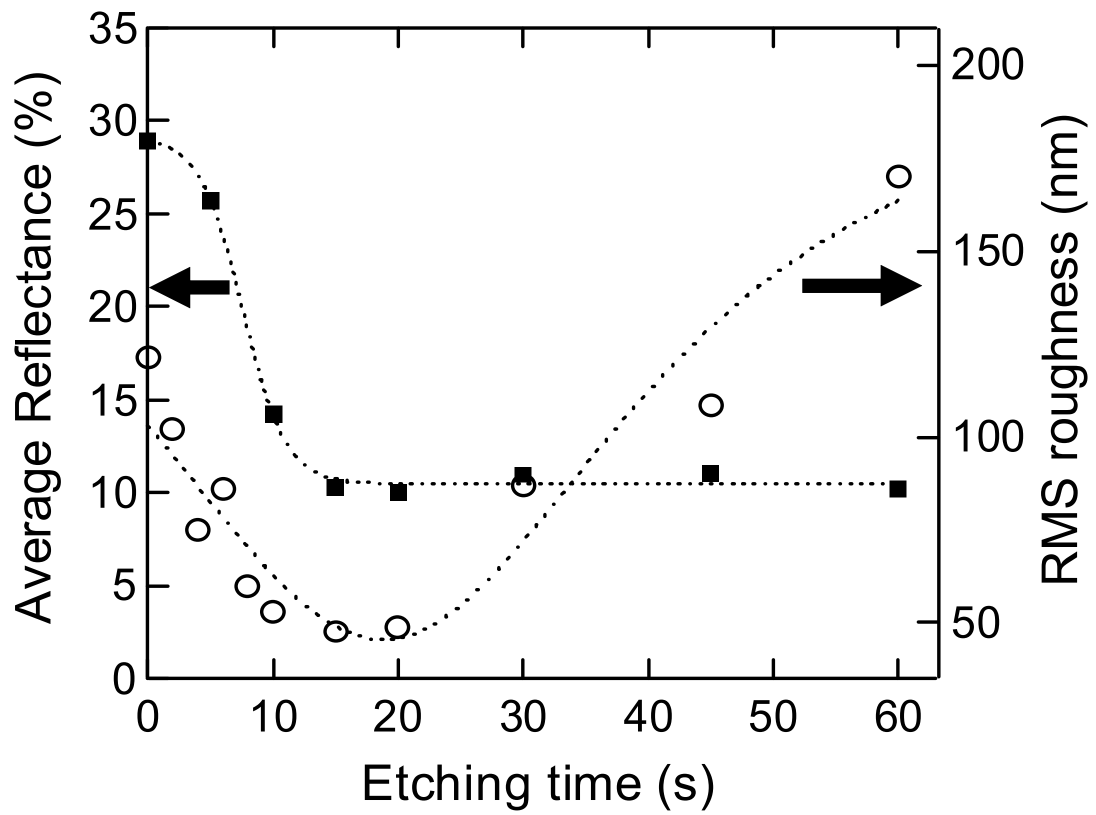

Figure 7 K. Ohdaira *et al*.,

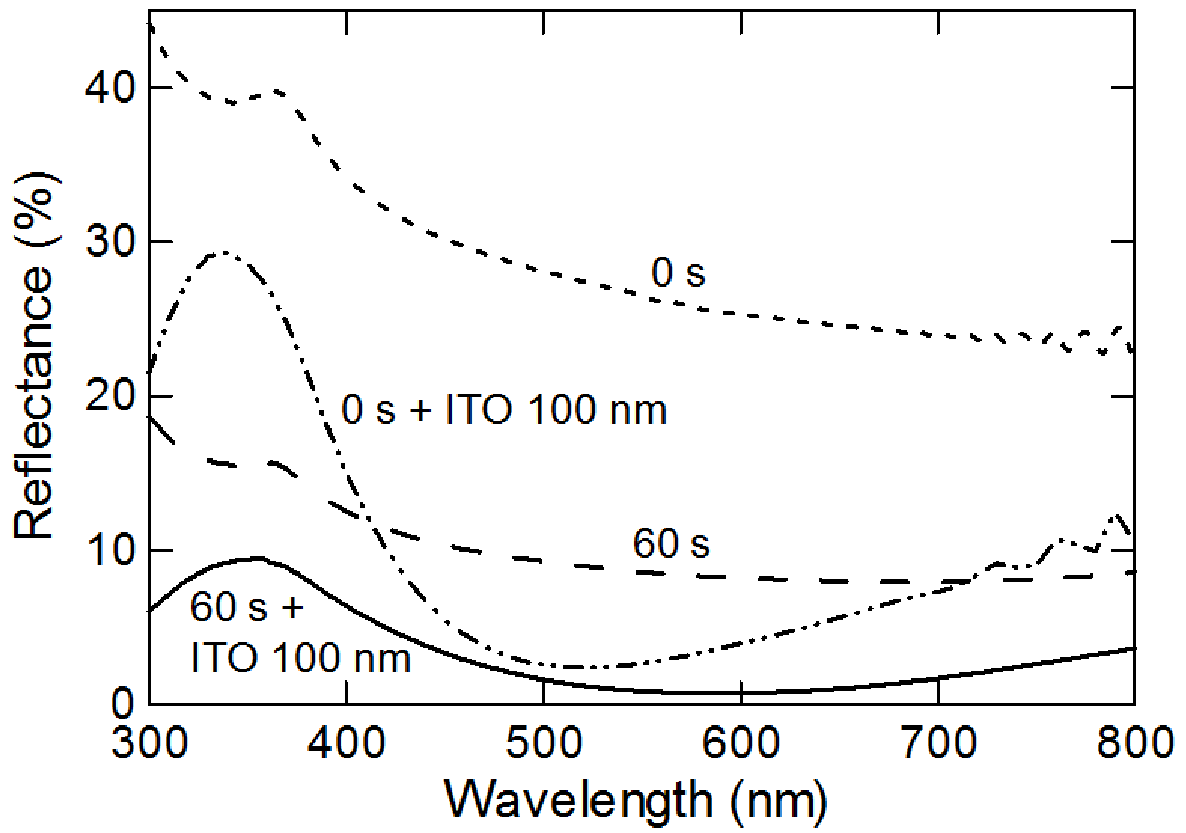

Figure 8 K. Ohdaira *et al.*,